

Reproducing the DAMA/LIBRA phase-2 results with two dark matter components

Juan Herrero-Garcia,^{1a,1} Andre Scaffidi,^{2a,2} Martin White,^{3a} and Anthony G. Williams,^{4a,3}

^aARC Centre of Excellence for Particle Physics at the Terascale, Department of Physics, University of Adelaide, Adelaide, South Australia 5005, Australia

E-mail: juan.herrero-garcia@adelaide.edu.au, andre.scaffidi@adelaide.edu.au, martin.white@adelaide.edu.au, anthony.williams@adelaide.edu.au

ABSTRACT: Recently the DAMA/LIBRA collaboration released the long-awaited phase-2 results with a lower energy threshold. It was recently argued that a one-component dark matter explanation of the observed annual modulation is strongly disfavoured or excluded unless isospin-violating couplings are invoked. In this short letter, we make the observation that dark matter comprising both a light and a heavy state can reproduce the observed spectrum without the need to invoke fine-tuned isospin-violating couplings. We perform a fit to scenarios with two-component dark matter and find that they are indeed in excellent agreement with the data. Our results show that two qualitatively different solutions are possible in the simplest case of isospin-conserving couplings with equal cross sections (or energy densities) of the two components. The p-values of the best-fit points of the two-component scenarios are equal, or better than, those of the one-component isospin-violating case. We also find very good agreement in the case of general two-component dark matter models.

KEYWORDS: Dark matter theory, dark matter experiments, direct detection, annual modulation, weakly interacting massive particles

ARXIV EPRINT: 1804:XXXX

¹<http://orcid.org/0000-0002-3300-0029>

²<http://orcid.org/0000-0002-1203-6452>

³<http://orcid.org/0000-0001-5474-4580>

⁴<http://orcid.org/0000-0002-1472-1592>

Contents

1	Introduction	1
2	The dark matter annual modulation signal	2
3	Fitting the full DAMA/LIBRA data set	4
3.1	Analysis methods	4
3.2	One-component dark matter	5
3.3	Two-component dark matter	5
4	Conclusions	8

1 Introduction

The nature of dark matter (DM) is one of the greatest mysteries of nature. Until now evidence for its existence stems from its gravitational interactions. There is one potential exception coming from direct detection experiments: the long-standing annual modulation signal observed by the DAMA/LIBRA collaboration [1, 2] (denoted by DAMA in the following). The significance for the annual modulation of the complete data set is 12.9σ . DAMA is unable to distinguish, on an event-by-event basis, electron recoils from nuclear recoils on its sodium iodide (NaI) crystals. However, by measuring the annual modulation (c.f., the total rate) and by performing different checks (only single hit events, phase close to June 2nd, period of 1 year, amplitude, etc.) the DAMA collaboration rejects the possibility that modulated backgrounds (neutrons, muons, solar neutrinos, radon, etc.) are the cause of the signal. Also several independent studies have been performed in the literature without finding any conclusive explanation [3–7]. Until the very latest phase-2 results, under reasonable particle physics and astrophysical assumptions the signal was consistent in both amplitude and phase with that expected from Weakly Interacting Massive Particles (WIMPs). Assuming the Standard Halo Model (SHM) and elastic scattering, the best-fit masses and cross sections are well-known: a light DM with mass ~ 10 GeV scattering mainly on sodium (light mass solution), or a heavy DM with mass ~ 70 GeV scattering mainly on iodine (heavy mass solution) [8–13].

The main issue with a DM interpretation of the DAMA modulation is that no other independent experiments have observed any DM signals, where compatibility with DAMA would require such signals to have been seen under currently understood physical particle and astrophysics scenarios. For example, LUX [14], XENON1T [15] and PandaX [16]) appear to exclude a DM origin of the DAMA observations. There is no currently accepted explanation that reconciles DAMA’s signal with the absence of results in all other experiments, e.g., see Refs. [10, 11, 17]. Furthermore, in the last few years halo-independent methods have been designed and applied to DAMA and appear to exclude a DM origin of the results independent of the assumed velocity distribution [18–24]. This

has motivated a large experimental effort to try to reproduce the DAMA experiment with NaI crystals in order to independently either confirm it or reject it [25–28]. The SABRE experiment plans to have a northern and southern hemisphere pair of NaI detectors to search for a seasonal correlation or anti-correlation of any DAMA-like annual modulation signal [29, 30].

Very recently, the DAMA collaboration released the long-awaited phase-2 results with a lower energy threshold, with the three new energy bins below 2 keVee [31]. With this new data the consistency of the DM interpretation of DAMA’s signal is under question both for the light and the heavy DM mass solutions mentioned above [32], even before having to consider its compatibility with other null results experiments. The issue is that, below 2 keVee the two standard DM solutions behave very differently with decreasing energy: the light DM would now give rise to scatterings in iodine, increasing its rate significantly in the case of spin-independent (SI) interactions, while for the heavy DM the modulation amplitude would decrease, approaching the phase flip. This was already pointed out in Ref. [33]. With the new data, it was shown in Ref. [32] and also confirmed below in this work, that the one-component spin-independent (SI) DM explanation of the annual modulation is disfavoured or excluded unless isospin-violating (IV) couplings are invoked. In particular, we find that the light DM solution is excluded at 5.3σ , while the heavy one is excluded at 3.0σ , in agreement with Ref. [32]. In the case of IV couplings, an adequately tuned destructive interference between the DM couplings to neutrons and protons can still correctly reproduce the spectrum by suppressing the interactions with iodine.

The main observation of this short letter is that the modulation amplitude observed by DAMA at low energies can be reproduced in a natural way by a combination of two DM particles, without the need to invoke fine-tuned IV couplings. As we will quantify explicitly below, two DM components give an excellent fit to the data for SI isospin-conserving (IC) couplings, equal to, or better than, that of the one-component scenario with IV couplings. From a theoretical perspective, it is also not difficult to envisage a dark sector, which accounts for 25% of the energy density of the Universe, to consist of more than one light stable state, similar to the way in which the visible sector (which accounts for only 5% of the energy budget) has a few stable particles: protons, electrons, the lightest neutrino, Helium nuclei, etc. Only a few works have studied the case of multi-component DM in direct detection, focusing on constant event rates [34–41]. In the following, we adopt a purely phenomenological approach to try to reproduce the observed modulated signal without going into further details regarding the model building, which would affect the interactions and the abundances of the DM components. This will be studied in a future work [42].

This letter is structured as follows. In Sec. 2 we introduce the relevant notation to describe the DM annual modulation signal in direct detection experiments. We discuss the fitting procedure used in Sec. 3.1. In Sec. 3.2 we show results of the fits of the vanilla one-component scenario with and without IV couplings to the full DAMA data set. We show the main results of this paper for two-component DM in Sec. 3.3. We present best-fit values and two-dimensional confidence level contours for two-component DM. This is done for the simplest case with IC couplings and also for the more general case with IV interactions. We give our conclusions and final remarks in Sec. 4.

2 The dark matter annual modulation signal

In this section, we present the relevant expressions for the direct detection of DM comprising two components with masses $m_{1,2}$ (we take $m_1 < m_2$ such that component 1 is always lighter than

component 2), SI cross-sections with protons $\sigma_{1,2}^p$, and local energy densities $\rho_{1,2}$. We impose the constraint $\rho_1 + \rho_2 = \rho_{\text{loc}}$, where ρ_{loc} is the observed DM mass density, which we fix to $0.4 \text{ GeV}/\text{cm}^3$. Following the notation of Ref. [41], it is useful to define the following ratios

$$r_\rho \equiv \frac{\rho_2}{\rho_1}, \quad r_\sigma \equiv \frac{\sigma_2^p}{\sigma_1^p}, \quad (1)$$

such that $\rho_2 = \rho_{\text{loc}} r_\rho / (1 + r_\rho)$. In this work, we will focus on the DM annual modulation signal [43, 44]. For the case of two-component DM, we can write the amplitude of the annual modulation rate in a detector with target nucleus labelled by (A, Z) , as (see for instance Refs. [13, 21, 22, 45]):

$$\begin{aligned} \mathcal{M}_A(E_R) &= \mathcal{M}_A^1(E_R) + \mathcal{M}_A^2(E_R) \\ &= \frac{x_A \rho_{\text{loc}} \sigma_1^p}{2(1+r_\rho) \mu_{p1}^2} F_A^2(E_R) \left(A_{\text{eff},1}^2 \frac{\delta\eta(v_{m,A}^{(1)})}{m_1} + r_\rho r_\sigma A_{\text{eff},2}^2 \frac{\mu_{p1}^2}{\mu_{p2}^2} \frac{\delta\eta(v_{m,A}^{(2)})}{m_2} \right). \end{aligned} \quad (2)$$

Here $F_A(E_R)$ is the SI nuclear form factor of element A , for which we will use the Helm parametrisation [46, 47]. x_A is the mass fraction of the target A in the detector. The total modulation amplitude is given by $\mathcal{M}(E_R) = \sum_A \mathcal{M}_A(E_R)$. The modulated rate for DM consisting of just one component is obtained from Eq. (2) in the limit $r_\rho = r_\sigma = 0$.

In the following we use the label $\alpha = 1, 2$ for the two DM components. In addition to the local energy densities, the astrophysics enters in Eq. (2) through the halo integral of the modulation

$$\delta\eta(v_{m,A}^{(\alpha)}) = \frac{1}{2} \left[\eta(v_{m,A}^{(\alpha)}, t_{\text{max}}) - \eta(v_{m,A}^{(\alpha)}, t_{\text{min}}) \right], \quad (3)$$

where t_{max} (t_{min}) are the times of the year where the velocity of the WIMP flow in the Earth's frame is maximum (minimum), which for minimum velocities above $\sim 200 \text{ kms}^{-1}$ corresponds to June (December) 2nd. Here we defined the halo integral as

$$\eta(v_{m,A}^{(\alpha)}, t) = \int_{v > v_{m,A}^{(\alpha)}} d^3v \frac{f_{\text{det}}^{(\alpha)}(\vec{v}, t)}{v} \quad \text{with} \quad v_{m,A}^{(\alpha)} = \sqrt{\frac{m_A E_R}{2\mu_{\alpha A}^2}}, \quad (4)$$

where $v_{m,A}^{(\alpha)}$ is the minimal velocity of the DM particle α required to produce a recoil of energy E_R in element A , and $f_{\text{det}}(\vec{v}, t)$ describes the distribution of DM particle velocities in the detector rest frame, which we assume to be equal for both DM species. It can be written in terms of the galactic velocity distributions by doing a Galilean boost, $f_{\text{det}}(\vec{v}, t) = f_{\text{gal}}(\vec{v} + \vec{v}_e(t))$, where $\vec{v}_e(t)$ is the velocity vector of the Earth in the galaxy rest-frame. We will use the SHM, with a Maxwellian velocity distribution

$$f_{\text{gal}}(\vec{v}) = \frac{1}{N_{\text{esc}}} \left(\frac{3}{2\pi\sigma_{H\alpha}^2} \right)^{3/2} \exp\left(-\frac{3\vec{v}^2}{2\sigma_{H\alpha}^2}\right), \quad (5)$$

with a cut-off at the escape velocity $v_{\text{esc}} = 550 \text{ km s}^{-1}$ and $N_{\text{esc}} = \text{erf}(z) - \frac{2}{\sqrt{\pi}} z e^{-z^2}$, where $z = \sqrt{3/2} v_{\text{esc}} / \sigma_{H\alpha}$. The velocity dispersion of each DM component, $\sigma_{H\alpha}$, may in principle be different. Indeed, if both components reach equilibrium in the halo, the velocity dispersions are expected to become mass dependent [48]. In this case one can write $\sigma_{H\alpha} = \bar{\sigma}_H \sqrt{\bar{m}/m_\alpha}$, where $\bar{m} = \sum n_\alpha m_\alpha / \sum n_\alpha$, with $n_\alpha = \rho_\alpha / m_\alpha$ the number density of the DM particle α , and $\bar{\sigma}_H \sim 270 \text{ kms}^{-1}$ is the canonical velocity dispersion. Throughout the paper we will generally assume equal velocity

dispersions for both components, $\sigma_{H_1} = \sigma_{H_2} = \bar{\sigma}_H$, but we will briefly discuss how our results change in the case in which they are given by the mass-dependent relationship provided above.

In order to properly fit a model to the DAMA data we must first take into account the finite energy resolution of the detector. This is done via the convolution of the theoretical modulation amplitude $\mathcal{M}(E_R)$ and the differential response function $\phi(E_R, E_{ee})$ ¹

$$M(E_{ee}) = \int_0^\infty dE_R \epsilon(E_{ee}) \phi(E_R, E_{ee}) \mathcal{M}(E_R), \quad (6)$$

where $\epsilon(E_{ee})$ is the detector efficiency and E_{ee} is the electron equivalent energy, related to the true recoil energy E_R through the target-dependent quenching factors $E_{ee} = Q_A E_R$. We use $Q_{\text{Na}} = 0.3$ and $Q_{\text{I}} = 0.09$ for the quenching factors of sodium and iodine. We also use the differential response function provided in Ref. [32], so that we can compare our results to the one-component case studied there. The modulation amplitude in bin i , M_i , is obtained by averaging the corrected modulation amplitude of Eq. 6 over each bin.

3 Fitting the full DAMA/LIBRA data set

In the next section, we briefly discuss details of our numerical scan and the data used. Afterwards, we show results of the fits to the one and the two-component DM scenarios in Secs. 3.2 and 3.3, respectively.

3.1 Analysis methods

In order to test the compatibility of a particular DM model with a given set of experimental data, one can employ the method of maximum likelihood. For the case of DAMA we parameterise the likelihood function with a binned Gaussian distribution:

$$\mathcal{L}(\vec{\mu} | \theta) = \prod_{i=1}^N \frac{1}{\sqrt{2\pi}\sigma_i} e^{-\frac{[\mu_i - M_i(\theta)]^2}{2\sigma_i^2}}, \quad (7)$$

where N is the number of bins and $M_i(\theta)$ is the expected modulation amplitude in bin i , defined below Eq. 6, which depends on different DM parameters denoted by $\theta = (\theta_1, \dots, \theta_n)$, where n is the total number of fitted parameters. μ_i is the central value of the observed annual modulation amplitude in bin i , and σ_i its error. Maximising the likelihood in Eq. (7) with respect to the parameters θ is equivalent to minimising -2 times the log-likelihood as follows:

$$\min_{\theta} (-2 \ln \mathcal{L}) = \min_{\theta} \sum_{i=1}^N \frac{[\mu_i - M_i(\theta)]^2}{\sigma_i^2} \equiv \min_{\theta} \chi^2(\theta). \quad (8)$$

This is the familiar *chi-square* test statistic which, as shown by Pearson [49], in the limit of large μ_i follows a χ^2 distribution with $N - n$ degrees of freedom (dof). Since the mean of a χ^2 distribution is the number of degrees of freedom (dof), the *goodness of fit* can be determined by the value of the χ^2 at the minimum, χ_{min}^2 , divided by the number of dof.

In our χ^2 fit we use the whole DAMA annual modulation data set, which combines results from DAMA/NaI and DAMA/LIBRA phases 1 and 2. The total exposure is 2.46 ton y. The results are

¹Note that the data presented by the DAMA collaboration is already corrected for the detector efficiency, so we conduct our analysis taking $\epsilon(E_{ee}) = 1$.

Parameter	Prior Range	Prior type
m_1	[1, 50] GeV	Flat
m_2	$[m_1, 1000]$ GeV	Flat
σ_p	$[10^{-42}, 10^{-38}]$ cm ²	Logarithmic
r_ρ	[0.001, 1000]	Logarithmic

Table 1: Parameters and prior ranges used for the two-component dark matter fits. In the four-dimensional fit, the four parameters are used with $\kappa_1 = \kappa_2 = r_\sigma = 1$.

provided in slide 22 of Ref. [31]. We use the data of Tab. I of Ref. [32], which gives the observed modulation amplitude M_i in $N = 10$ bins in the energy range [1, 20] keVee.

We use the open source software `Minuit` [50] to compute the best-fit points, which we give in Tabs. 2 and 3. For completeness, we will also compute the corresponding p-values for the fits, as well as the corresponding number of equivalent two-sided Gaussian standard deviations \mathcal{Z} . We consider a ‘good’ fit as one that yields a p-value $> 1 \times 10^{-3}$, which corresponds to $\mathcal{Z} < 1.96$. Of course, this is to some extent an arbitrary choice. For the two-component scenarios, we also employ the `MultiNest` implementation of the nested sampling algorithm [51–53]. The latter is well suited for dealing with a highly multimodal target function, which as we will see is the case for two-component scenarios. We will show results with 10^4 live points and a tolerance of 0.01. For the two-component DM fits we use the priors shown in Tab. 1. We determine the distribution of the profile likelihood ratio (PLR) $\mathcal{L}/\mathcal{L}_{\max}$ throughout the parameter space from the obtained samples, and derive the frequentist 1 and 2σ C.L. contours using `pippi` [54].²

3.2 One-component dark matter

We perform fits of one-component DM (1DM) to the DAMA data. We do this for SI interactions with both IC and IV couplings. The former scenario involves just 2 free parameters, while the latter has 3. We show the results for the light and the heavy DM mass solutions. In Tab. 2 we show the best-fit points obtained, as well as the values of χ_{\min}^2/dof , the p-values and Z . As can be observed, unless IV couplings are invoked, there is no good fit to DAMA.

It is quite easy to visualise how a combination of both light and heavy DM could give a spectrum that could reproduce the observed signal in the lowest energy bins. This is the main idea of this paper, which will be studied in the next section.

3.3 Two-component dark matter

In this section we perform a fit of the annual modulation amplitude generated by two DM particles (2DM) to the DAMA data. We first take IC couplings and fix $r_\sigma = 1$, leaving r_ρ free. These models have 4 free parameters. The energy density and the cross section enter identically in the

²We have checked the consistency of the best-fit points obtained with `MultiNest` and with `Minuit` by adequately choosing the search ranges in the latter. The reason is that `MultiNest` is well suited to finding different local minima in multi-dimensional parameter spaces, but, unless a very low tolerance and a high efficiency are used, which would make the scans very computationally expensive, the best-fit points may not be as accurate as those given by `Minuit`. Therefore in the tables we show those obtained with the latter.

1DM	m	σ_1^p	κ	χ_{\min}^2/dof	p-value	\mathcal{Z}
IC light	8.40	1.25	-	48.0/8	1.0×10^{-7}	5.3
IC heavy	54.0	0.058	-	23.1/8	3.2×10^{-3}	3.0
IV light	10.9	75.8	-0.67	12.1/7	0.10	1.7
IV heavy	50.4	30.0	-0.65	13.1/7	0.07	1.8

Table 2: Results of the one-component dark matter fit to DAMA data. The DM mass m is in GeV and the scattering cross section with protons σ_1^p is in units of 10^{-40} cm^2 . The different fits are for both the light and the heavy dark matter mass solutions, which correspond to scatterings mainly in Na and I, respectively. We show isospin-conserving (IC) and isospin-violating (IV) couplings. The dashes refer to the parameters that are fixed to 1 and therefore are not varied in the fit. The last two columns provide the p-value and the number of Gaussian-equivalent standard deviations \mathcal{Z} (two-sided).

2DM	m_1	m_2	σ_1^p	r_ρ	r_σ	κ_1	κ_2	χ_{\min}^2/dof	p-value	\mathcal{Z}
IC A	19.8	76.1	0.13	3.04	-	-	-	10.7/6	0.10	1.7
IC B	8.19	170	2.55	0.07	-	-	-	9.17/6	0.16	1.4
IV general	17.8	70.7	5.84	32.2	1.15	0.03	-0.52	7.80/3	0.05	2.0

Table 3: Same as Tab. 2 for the two-component dark matter fit to DAMA data. The different fits are performed for the isospin-conserving (IC) simplified case (first two rows), as well as in the most general isospin-violation (IV) one (last row). Two solutions, A and B, exist in the case of IC couplings.

rate, $\mathcal{M} \propto \rho_\alpha \sigma_\alpha$. Therefore, apart from the overall normalisation, one can fix r_σ and consider r_ρ as a free parameter. We have also checked that the other scenario (fixing $r_\rho = 1$ and leaving r_σ free) gives a similar fit with a cross section that is roughly twice that of the case of $r_\sigma = 1$ because $r_\rho \simeq 3$, confirming the expectations. We then do a general fit with free r_ρ and r_σ and IV couplings, which involves 7 free parameters.

We show in Tab. 3 the results of the fits of two-component DM (2DM) to the annual modulation signal observed by DAMA. We show the best-fit points of the different fits performed, as well as the values of χ_{\min}^2/dof , the p-values and the Gaussian-equivalent number of standard deviations \mathcal{Z} . In the first two rows we show the two IC best-fit solutions, while in the last one we show the more general case of IV ones. For IC couplings two solutions exist. One can observe that solution B, with the larger mass splitting between the two DM particles, is a better fit than solution A. Although the general IV model (last row) produces a smaller χ_{\min}^2 than both IC cases, its larger number of free parameters yields a smaller p-value and hence a worse fit. Therefore, in the following we will only focus on the four-parameter IC cases.

Let us also briefly mention how our results change in the case of mass-dependent velocity dispersions. To investigate their impact, we performed a dedicated Minuit fit around the parameters given by the IC solution A in Tab. 3, in which the velocity dispersions were allowed to be

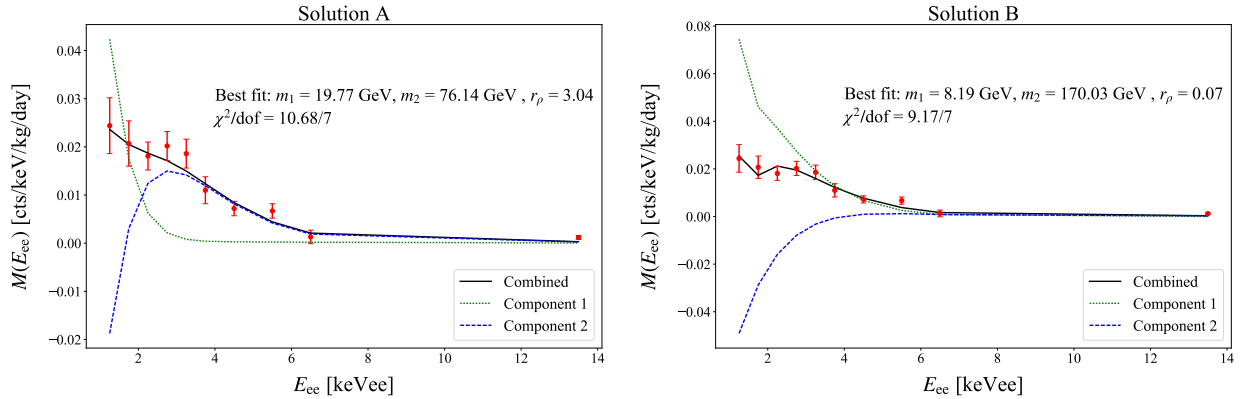


Figure 1: Best-fit spectra for a two-component dark matter model with isospin-conserving couplings (solid black line). Two solutions are possible, A (*left panel*) and B (*right panel*). The DAMA experimental results are shown as red points. We also show the individual contributions in dotted green (component 1) and dashed blue (component 2).

mass-dependent. We obtain $\chi_{\min}^2/\text{dof} = 10.69$, with best-fit values $m_1 = 19.66$ GeV, $m_2 = 75.8$, $\sigma_1^p = 0.13$ and $r_\rho = 3.02$. Therefore, the results are very similar to the mass-independent velocity-dispersion case.

In Fig. 1 we show with a solid black line the binned modulation amplitude for the best-fit points for two-component DM in the case of IC couplings for solution A (left panel) and solution B (right panel). We also show the individual contributions in dotted green (component 1) and dashed blue (component 2), and the DAMA experimental results as red points. We have checked that solution A corresponds to scattering of both DM components *dominantly* off iodine. The fact that the lighter component scatters dominantly off iodine with a negligible contribution from sodium is due to two factors: first, the smaller quenching factor in iodine compensates its larger mass, translating into smaller $v_{m,1}^{(1)}(E_R)$ and thus into larger $\eta(v_{m,1}^{(1)})$; second, the A^2 enhancement factor for iodine. For this solution, component 1 dominates for energies roughly below 2 keVee. On the other hand, for solution B, component 2 scatters off iodine for all shown recoil energies, while component 1 scatters off sodium above roughly 2 keVee, with a significant contribution from iodine scatterings below that energy, which explains the observed rapid increase in its spectrum at low energies. For this solution, component 1 always has a larger modulation amplitude than component 2. As expected in the SHM, the phase flip for the heavy state (component 2) occurs at an electron equivalent energy E_{ee} approximately equal to 1.6 (3.6) keVee for solution A (B).

In Fig. 2 we show the profile likelihood ratio (PLR) density $\mathcal{L}/\mathcal{L}_{\max}$ overlaid with 1 and 2σ C.L. contours. We only show four illustrative slices of the full four dimensional parameter space. One will immediately notice two distinct regions of high PLR density which correspond to the two solutions A and B, which we indicate in the plot. There is a slight preference for solution B (see Tab. 3). One can observe that the 1 and 2σ regions are quite extended, with a significant range of parameters being able to reproduce the DAMA results.

In the m_1 - m_2 plane (*top left panel*) one can observe that, for each of the solutions, one of the DM components has a narrow range of masses (for example component 1 for solution B, which always gives the largest contribution at all energies) while the other one (component 2 for solution B) spans a large mass range, with a contribution that is subdominant. There is a sizable range of

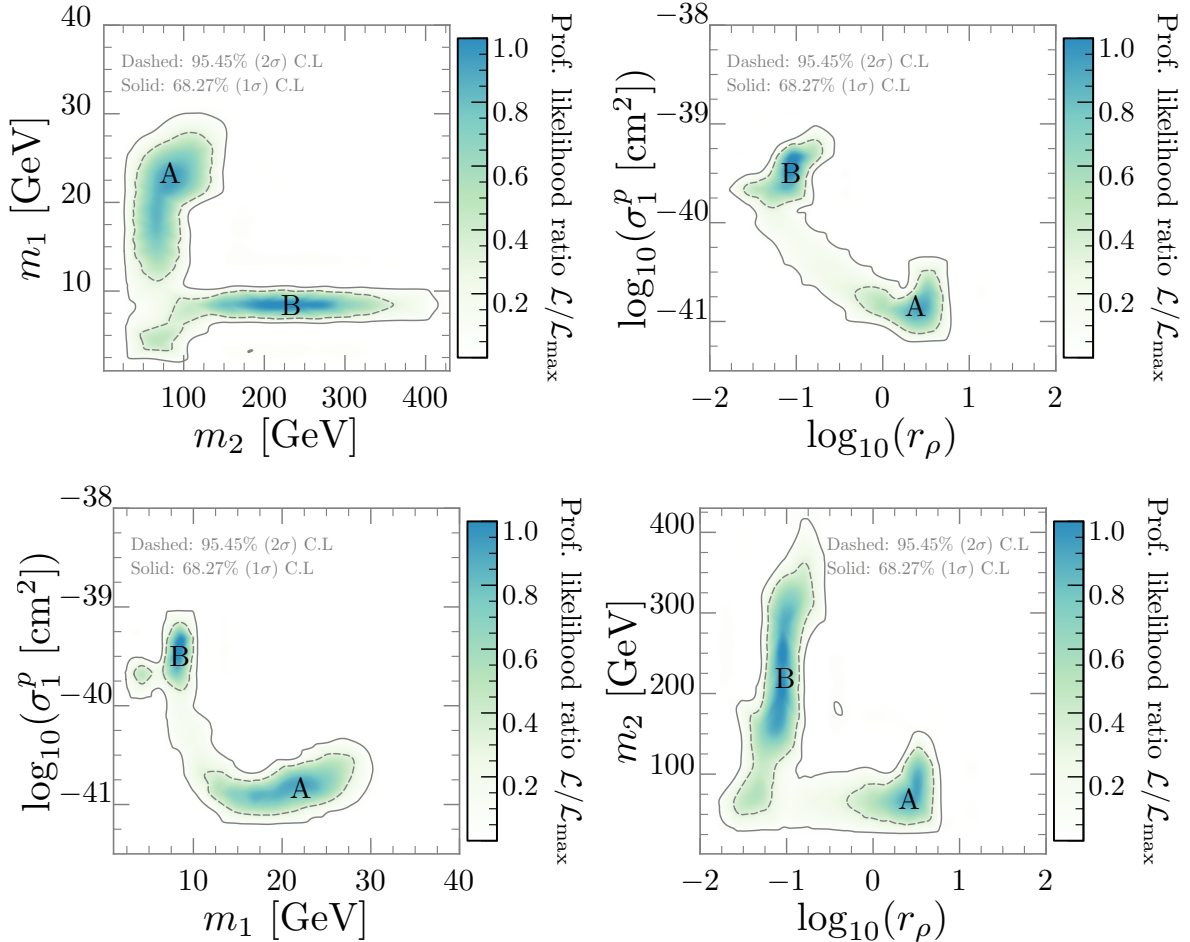


Figure 2: Profile likelihood ratio (PLR) density overlaid with 1 and 2σ C.L. contours for the two-component isospin-conserving dark matter fit to DAMA data. We show four illustrative two-dimensional slices of the four-dimensional parameter space. We indicate the two distinct regions of high PLR density corresponding to the two best-fit solutions A and B (see Tab. 3.)

mass splittings that provide a good fit. In the $\log_{10}(r_\rho)$ - $\log_{10}(\sigma_1^p)$ plane (*top right panel*) one can observe that the two solutions are aligned in a band with negative correlation, i.e., the larger the cross section the smaller the ratio of energy densities.³ In the $\log_{10}(r_\rho)$ - m_2 plane (*bottom left panel*) we see that it is solution B (with lighter m_1 and heavier m_2) that has the larger cross section. In the $\log_{10}(r_\rho)$ - m_2 plane (*bottom right panel*) the large degeneracy in the case of solution B between m_2 and r_ρ is clearly visible. It is due to the fact that, for $m_2 \gg m_I$, the minimum velocity of the second component in iodine, $v_{m,I}^{(2)}$, approaches a constant value, so that its contribution to the amplitude only depends on the ratio r_ρ/m_2 .

4 Conclusions

The observed annual modulation in the low energy bins below 2 keVee in the Phase-2 run DAMA/LIBRA results is no longer compatible with a one-component dark matter interpretation in the simplest spin-independent isospin-conserving scenario. The reason is easy to understand: a light

³Therefore the figures in the $\log_{10}(r_\rho)$ - m_1 and the m_2 - $\log_{10}(\sigma_1^p)$ planes can be easily obtained from the ones in Fig. 2 and we do not show them.

DM particle that predominantly scatters off sodium produces a spectrum that steeply increases at lower recoil energy due to iodine scatterings becoming allowed; conversely, a high DM mass produces a spectrum that falls off at the lowest energy bins. The issue is that the observed values in the lowest energy bins happen to lie, roughly speaking, between the expected spectrum of a light and that of a heavy DM state. It then seems natural that a two-component model comprising both a light and heavy component can revive the DM interpretation of the low threshold data. Of course, the relative local energy densities, namely r_ρ (or similarly, the relative strength of their interactions, r_σ) should play an important role in the compatibility of the two-component explanation.

In this short letter we performed a fit of two-component DM to DAMA data. Contrary to the case of one-component DM where now only IV couplings provide a good fit, we find very good agreement to the data also for IC couplings. Two different solutions with qualitatively different spectral behaviour are found, shown in Fig. 1. On one of them (A), scatterings are predominantly on iodine, with a crossing between the spectrum of the two individual DM components at roughly 2 keVee. On the other one (B), the lighter component scatters off both sodium and iodine at the lowest energies and the individual spectra do not cross. The results of the fits are summarised in Tab. 3 and Fig. 2, which involve reasonable values of the relative energy densities and the cross section. Although model-dependent assumptions regarding the velocity dispersions or the relic abundance of the different DM components may modify the results, the main conclusions are expected to hold, that is, that the DAMA spectrum can be well reproduced by two DM particles.⁴

Two-component DM therefore looks like a natural solution to the first part of the DAMA puzzle: the compatibility of the spectrum with that expected from DM under standard astrophysical and particle physics assumptions. The second part of the DAMA puzzle, that is, the compatibility of DAMA data with other null results is not solved. It is interesting to speculate, however, how it might be somewhat improved in the scenario considered here.

Acknowledgements:

This work is supported by the Australian Research Council through the Centre of Excellence for Particle Physics at the Terascale CE110001004. MW is supported by the Australian Research Council Future Fellowship FT140100244. MW wishes to thank Lucien Boland and Sean Crosby for their administration of, and ongoing assistance with, the MPI-enabled computing cluster on which this work was performed.

References

- [1] DAMA, LIBRA, R. Bernabei *et al.*, *New results from DAMA/LIBRA*, Eur. Phys. J. **C67**, 39 (2010), 1002.1028.

⁴In this work we focused on the amplitude of the annual modulation. Let us also mention that the phase of the modulation is also sensitive to the DM mass via gravitational focusing, and thus in theory also to the existence of one or two DM components, and to their masses. Although this effect is expected to be small [55–57], it would be interesting to study it in more detail.

- [2] R. Bernabei *et al.*, *Final model independent result of DAMA/LIBRA-phase1*, Eur. Phys. J. **C73**, 2648 (2013), 1308.5109.
- [3] E. Fernandez-Martinez and R. Mahbubani, *The Gran Sasso muon puzzle*, JCAP **1207**, 029 (2012), 1204.5180.
- [4] J. Klinger and V. A. Kudryavtsev, *Can muon-induced backgrounds explain the DAMA data?*, J. Phys. Conf. Ser. **718**, 042033 (2016).
- [5] P. Belli *et al.*, *Search for double beta decay in ^{106}Cd in the DAMA/CRYSTAL setup*, AIP Conf. Proc. **1894**, 020005 (2017).
- [6] R. Bernabei and F. Cappella, *Investigation of rare nuclear decays with the DAMA set-ups*, Int. J. Mod. Phys. **A33**, 1843005 (2018).
- [7] D. N. McKinsey, *Is DAMA Bathing in a Sea of Radioactive Argon?*, (2018), 1803.10110.
- [8] P. Gondolo and G. Gelmini, *Compatibility of DAMA dark matter detection with other searches*, Phys. Rev. **D71**, 123520 (2005), hep-ph/0504010.
- [9] M. Fairbairn and T. Schwetz, *Spin-independent elastic WIMP scattering and the DAMA annual modulation signal*, JCAP **0901**, 037 (2009), 0808.0704.
- [10] J. Kopp, T. Schwetz, and J. Zupan, *Global interpretation of direct Dark Matter searches after CDMS-II results*, JCAP **1002**, 014 (2010), 0912.4264.
- [11] T. Schwetz and J. Zupan, *Dark Matter attempts for CoGeNT and DAMA*, JCAP **1108**, 008 (2011), 1106.6241.
- [12] E. Del Nobile, G. B. Gelmini, A. Georgescu, and J.-H. Huh, *Reevaluation of spin-dependent WIMP-proton interactions as an explanation of the DAMA data*, JCAP **1508**, 046 (2015), 1502.07682.
- [13] J. Herrero-Garcia, *Halo-independent tests of dark matter annual modulation signals*, JCAP **1509**, 012 (2015), 1506.03503.
- [14] LUX, D. S. Akerib *et al.*, *Results from a search for dark matter in the complete LUX exposure*, Phys. Rev. Lett. **118**, 021303 (2017), 1608.07648.
- [15] XENON, E. Aprile *et al.*, *First Dark Matter Search Results from the XENON1T Experiment*, (2017), 1705.06655.
- [16] PandaX-II, X. Cui *et al.*, *Dark Matter Results From 54-Ton-Day Exposure of PandaX-II Experiment*, Phys. Rev. Lett. **119**, 181302 (2017), 1708.06917.
- [17] C. Savage, G. Gelmini, P. Gondolo, and K. Freese, *XENON10/100 dark matter constraints in comparison with CoGeNT and DAMA: examining the L_{eff} dependence*, Phys. Rev. **D83**, 055002 (2011), 1006.0972.
- [18] C. McCabe, *DAMA and CoGeNT without astrophysical uncertainties*, Phys. Rev. **D84**, 043525 (2011), 1107.0741.

- [19] M. T. Frandsen *et al.*, *On the DAMA and CoGeNT Modulations*, Phys. Rev. **D84**, 041301 (2011), 1105.3734.
- [20] M. T. Frandsen, F. Kahlhoefer, C. McCabe, S. Sarkar, and K. Schmidt-Hoberg, *Resolving astrophysical uncertainties in dark matter direct detection*, JCAP **1201**, 024 (2012), 1111.0292.
- [21] J. Herrero-Garcia, T. Schwetz, and J. Zupan, *Astrophysics independent bounds on the annual modulation of dark matter signals*, Phys. Rev. Lett. **109**, 141301 (2012), 1205.0134.
- [22] J. Herrero-Garcia, T. Schwetz, and J. Zupan, *On the annual modulation signal in dark matter direct detection*, JCAP **1203**, 005 (2012), 1112.1627.
- [23] N. Bozorgnia, J. Herrero-Garcia, T. Schwetz, and J. Zupan, *Halo-independent methods for inelastic dark matter scattering*, JCAP **1307**, 049 (2013), 1305.3575.
- [24] G. B. Gelmini, J.-H. Huh, and S. J. Witte, *Assessing Compatibility of Direct Detection Data: Halo-Independent Global Likelihood Analyses*, JCAP **1610**, 029 (2016), 1607.02445.
- [25] J. Amaré *et al.*, *From ANAIS-25 towards ANAIS-250*, Phys. Procedia **61**, 157 (2015), 1404.3564.
- [26] PICO-LON, K. Fushimi *et al.*, *Dark matter search project PICO-LON*, J. Phys. Conf. Ser. **718**, 042022 (2016), 1512.04645.
- [27] G. Angloher *et al.*, *The COSINUS project - perspectives of a NaI scintillating calorimeter for dark matter search*, Eur. Phys. J. **C76**, 441 (2016), 1603.02214.
- [28] COSINE-100, W. G. Thompson, *Current status and projected sensitivity of COSINE-100*, in *15th International Conference on Topics in Astroparticle and Underground Physics (TAUP 2017) Sudbury, Ontario, Canada, July 24-28, 2017*, 2017, 1711.01488.
- [29] E. Shields, J. Xu, and F. Calaprice, *SABRE: A New NaI(Tl) Dark Matter Direct Detection Experiment*, Phys. Procedia **61**, 169 (2015).
- [30] SABRE, F. Froberg, *SABRE: WIMP modulation detection in the northern and southern hemisphere*, J. Phys. Conf. Ser. **718**, 042021 (2016), 1601.05307.
- [31] D. C. R. Bernabei, <https://agenda.infn.it/conferenceDisplay.py?confId=15474>, LNGS Scientific Committee Meeting (March 2018).
- [32] S. Baum, K. Freese, and C. Kelso, *Dark Matter implications of DAMA/LIBRA-phase2 results*, (2018), 1804.01231.
- [33] C. Kelso, P. Sandick, and C. Savage, *Lowering the Threshold in the DAMA Dark Matter Search*, JCAP **1309**, 022 (2013), 1306.1858.
- [34] S. Profumo, K. Sigurdson, and L. Ubaldi, *Can we discover multi-component WIMP dark matter?*, JCAP **0912**, 016 (2009), 0907.4374.
- [35] B. Batell, M. Pospelov, and A. Ritz, *Direct Detection of Multi-component Secluded WIMPs*, Phys. Rev. **D79**, 115019 (2009), 0903.3396.

- [36] A. Adulpravitchai, B. Batell, and J. Pradler, *Non-Abelian Discrete Dark Matter*, Phys. Lett. **B700**, 207 (2011), 1103.3053.
- [37] K. R. Dienes, J. Kumar, and B. Thomas, *Direct Detection of Dynamical Dark Matter*, Phys. Rev. **D86**, 055016 (2012), 1208.0336.
- [38] D. Chialva, P. S. B. Dev, and A. Mazumdar, *Multiple dark matter scenarios from ubiquitous stringy throats*, Phys. Rev. **D87**, 063522 (2013), 1211.0250.
- [39] S. Bhattacharya, P. Poulose, and P. Ghosh, *Multipartite Interacting Scalar Dark Matter in the light of updated LUX data*, JCAP **1704**, 043 (2017), 1607.08461.
- [40] S. Bhattacharya, P. Ghosh, T. N. Maity, and T. S. Ray, *Mitigating Direct Detection Bounds in Non-minimal Higgs Portal Scalar Dark Matter Models*, JHEP **10**, 088 (2017), 1706.04699.
- [41] J. Herrero-Garcia, A. Scaffidi, M. White, and A. G. Williams, *On the direct detection of multi-component dark matter: sensitivity studies and parameter estimation*, JCAP **1711**, 021 (2017), 1709.01945.
- [42] J. Herrero-Garcia, A. Scaffidi, M. White, and A. G. Williams, *Relic abundance implications on the direct detection of multi-component dark matter*, In preparation (2018).
- [43] A. K. Drukier, K. Freese, and D. N. Spergel, *Detecting Cold Dark Matter Candidates*, Phys. Rev. **D33**, 3495 (1986).
- [44] K. Freese, J. A. Frieman, and A. Gould, *Signal Modulation in Cold Dark Matter Detection*, Phys. Rev. **D37**, 3388 (1988).
- [45] K. Freese, M. Lisanti, and C. Savage, *Colloquium: Annual modulation of dark matter*, Rev. Mod. Phys. **85**, 1561 (2013), 1209.3339.
- [46] J. Lewin and P. Smith, *Review of mathematics, numerical factors, and corrections for dark matter experiments based on elastic nuclear recoil*, Astroparticle Physics **6**, 87 (1996).
- [47] R. H. Helm, *Inelastic and Elastic Scattering of 187-Mev Electrons from Selected Even-Even Nuclei*, Phys. Rev. **104**, 1466 (1956).
- [48] R. Foot, *Hidden sector dark matter explains the DAMA, CoGeNT, CRESST-II and CDMS/Si experiments*, Phys. Rev. **D88**, 025032 (2013), 1209.5602.
- [49] K. Pearson, *X. On the criterion that a given system of deviations from the probable in the case of a correlated system of variables is such that it can be reasonably supposed to have arisen from random sampling*, Philosophical Magazine **50**, 157 (1900).
- [50] F. James, *MINUIT Function Minimization and Error Analysis: Reference Manual Version 94.1*, (1994).
- [51] F. Feroz, M. P. Hobson, and M. Bridges, *MultiNest: an efficient and robust Bayesian inference tool for cosmology and particle physics*, Mon. Not. Roy. Astron. Soc. **398**, 1601 (2009), 0809.3437.

- [52] F. Feroz and M. P. Hobson, *Multimodal nested sampling: an efficient and robust alternative to MCMC methods for astronomical data analysis*, Mon. Not. Roy. Astron. Soc. **384**, 449 (2008), 0704.3704.
- [53] F. Feroz, M. P. Hobson, E. Cameron, and A. N. Pettitt, *Importance Nested Sampling and the MultiNest Algorithm*, (2013), 1306.2144.
- [54] P. Scott, *Pippi - painless parsing, post-processing and plotting of posterior and likelihood samples*, Eur. Phys. J. Plus **127**, 138 (2012), 1206.2245.
- [55] M. S. Alenazi and P. Gondolo, *Phase-space distribution of unbound dark matter near the Sun*, Phys. Rev. **D74**, 083518 (2006), astro-ph/0608390.
- [56] S. K. Lee, M. Lisanti, A. H. G. Peter, and B. R. Safdi, *Effect of Gravitational Focusing on Annual Modulation in Dark-Matter Direct-Detection Experiments*, Phys. Rev. Lett. **112**, 011301 (2014), 1308.1953.
- [57] N. Bozorgnia and T. Schwetz, *Is the effect of the Sun's gravitational potential on dark matter particles observable?*, JCAP **1408**, 013 (2014), 1405.2340.